Contents lists available at SciVerse ScienceDirect

CIRP Annals Manufacturing Technology

Journal homepage: www.elsevier.com/locate/cirp

Porosity testing methods for the quality assessment of selective laser melted parts

Wessel W. Wits[a], Simone Carmignato[b] (2), Filippo Zanini[b] and Tom H.J. Vaneker[a] (2)

[a] *Laboratory of Design, Production and Management, Faculty of Engineering Technology, University of Twente, Enschede, The Netherlands*
[b] *University of Padua, Department of Management and Engineering, Stradella San Nicola 3, Vicenza, Italy*

This study focuses on the comparison of porosity testing methods for the quality assessment of selective laser melted parts. Porosity is regarded as important quality indicator in metal additive manufacturing. Various destructive and non-destructive testing methods are compared, ranging from global to local observation techniques and from quick low-cost to expensive time-consuming analyses. Forty test specimens were produced using five varying control factors. The experimental results show that Archimedes and CT methods compare well, Archimedes can be deployed to inspect parts in small series and CT pre- and post-cut analysis show that post-cut porosity results are systematically higher.

Selective laser melting (SLM), Quality assurance, Porosity analysis

1. Introduction

Additive Manufacturing (AM) is seen as the core technology for future high-value engineered products and is expected to change the landscape of industrial production in the coming years [1-2]. It has tremendous potential for producing complex, individually customized parts in small-scale series [3]; however, standardized guidelines and methods for quality assurance and verification need to be developed [4]. Qualification approaches based on validated models and probabilistic methods are sought, as part-by-part inspection is time consuming and costly [5].

This study focuses on Selective Laser Melting (SLM) as metal-based AM technology for its versatility and capability to produce near full-dense parts. SLM produces parts by melting powder particles in a layer selectively, layer by layer successively. Final part properties strongly depend on the in-layer scan strategy and the layer-to-layer properties [6-7]. Although SLM is capable of building high-density parts close to the nominal density, due to process instabilities gas bubbles, oxides and unmolten particles may be entrapped [8-10]. Pores cannot be avoided completely and may act as nuclei for cracks leading to possible reduced mechanical properties [11]. Moreover, the morphology of the pores is related to the type of defect [12]. Relatively spherical pores are an indication of entrapped gas typically due to local overheating. In contrast, irregular elongated pores are an indication of unmolten particles typically due to insufficient energy (e.g. hatch pattern defects). Finally, the distribution and location of pores are indicative for the process conditions, and are therefore also useful information for quality assessment.

For part manufacture in general, SLM is still relatively expensive; therefore, one-off (high-value) products are more economically feasible than large series production. Hence, non-destructive testing methods are more favourable. To assess part quality, measuring part density or part porosity is essential [13]. In this paper, several methods for porosity detection are tested and compared: non-destructive methods such as Archimedes method, gas pycnometry and X-ray Computed Tomography (CT), as well as destructive methods as microscopic cross-section analysis. Archimedes and gas pycnometry are not capable of analysing fundamental porosity characteristics, while microscopic micrographs only allow investigation on a limited number of 2D cross-sections. On the other hand, CT has the potential to quantitatively evaluate the entire part for total pore volume, pore morphology, and pore distribution and location.

2. Testing methods

To validate the mechanical part performances for static loading conditions tensile testing is performed. Three responses are recorded, namely, yield strength, ultimate tensile strength and the Young's modulus. Advantages of this method are that it is well established, relatively inexpensive and easy to perform, and it is a good way to compare part (and material) properties in an experimental design. It is however a destructive method.

2.1. Density-based testing methods

Two density-based testing methods are studied: Archimedes method and gas pycnometry.

The Archimedes method is based on the difference in buoyancy of an object's weight measured in air and submerged into a fluid. Advantages of the Archimedes method are that it is non-destructive, relatively inexpensive and quick. It can however only be used to determine a global density value relative to the reference fluid. In this study, ethanol is used as the reference fluid and a Sartorius R200D electronic semi-microbalance is used to measure the weight. To compute the part porosity, the measured density has to be compared to the material's nominal reference density. A lower density value results from increased part porosity. Localized porosities, due to e.g. process instabilities, can however not be assessed individually. Internal defects should be closed not allowing fluid to infiltrate the submerged part.

In gas pycnometry, a pycnometer computes part density in an absolute sense by measuring part volume and part mass separately. Part volume is determined by gas displacement. In this study, a Micromeritics AccuPyc II 1340 Helium Pycnometer is used. Advantages of gas pycnometry are similar to the Archimedes method, although the equipment is a bit more expensive. The downside is the limited detection volume, allowing only relatively small parts to be measured. Analogously, only a global part density is measured, part porosity is computed by correlating a nominal reference density, and localized defects cannot be detected individually.

2.2. Porosity-based testing methods

In addition to the described density-based testing methods, two porosity-based testing methods are studied as well: microscopic analysis of cross-sections and X-ray CT.

In the first method, the sample is cut, embedded in epoxy resin, grinded, sanded with abrasive paper and finally polished, using Struers ApS equipment. A Zeiss Axioplan 2 microscope is used in this work to capture micrographs that are analysed by Axiovision image processing software capable of automatic image stitching. A pre-elaboration of the image is required to remove any residual scratch of the polishing procedure and to get a binarized image after the selection of an appropriate threshold value. The porosity percentage can be calculated as the ratio between black pixels count and white pixels count, while the pore's area can be evaluated by knowing the pixel size of the image. This testing method allows for the assessment of pore size and distribution, giving more information than the density-based methods, but confined to specific sections of the specimen. Thus, for non-homogeneous distributions of pores, the obtained results are not representative of the entire part. However, the most relevant disadvantage is the destructive nature of this method together with the high cost in terms of material and time usage.

The second method, X-ray CT, has been recently utilized as innovative non-destructive measuring technique for internal porosity detection thanks to its capability of providing a complete analysis of size, shape, volume and distribution of pores/defects within the entire analysed volume [14]. During a CT scan, a set of 2D X-ray projections is acquired at various angles as the sample, placed on a rotating stage and irradiated with an X-ray beam, rotates around the rotary axis. These projections are then used to reconstruct a 3D voxel (volumetric pixel) model of the sample, by means of a filtered back-projection algorithm [15]. Advanced segmentation algorithms can be applied after setting a grey value threshold to discriminate between air and the object material [16], and information about internal porosity can be extracted. Up to now, the most relevant drawbacks are the high cost and the high time usage. Moreover, the establishment of metrological traceability of CT porosity measurements is still a challenging task [17]. CT scanning was done using a metrological CT system (Nikon X-Tek MCT225) equipped with a 225 kV micro-focus X-ray source (min. focal spot size 3 µm), 2000x2000 flat panel detector (16 bit) and cabinet temperature controlled at 20 °C. CT volumes reconstructed in this work have a voxel size of $(9\ \mu m)^3$. The total CT porosity volume is measured using a threshold algorithm implemented in the software package VGStudio MAX 2.2.

3. SLM test part production

Following an experimental design, 40 tensile test specimens are produced and systematically analysed using the aforementioned testing methods. Five process factors were varied in the SLM build process (see Table 1). For Factors 1-4, the centre point values are based on the standard process parameter settings. The step-size variation was chosen such to trigger distinguishable process responses and are therefore not always considered optimal process settings. Factor no. 5 determines the build orientation: one set of test specimens was oriented horizontally; the other set was oriented vertically with respect to the platform.

Table 1. Control factors variation for the SLM build process.

No.	Factor	low	centre	high
1	Laser power [W]	150	225	300
2	Energy Density [J/mm³]	50	60	70
3	Focus offset [mm]	-3	2	7
4	Hatch distance [mm]	0.09	0.12	0.15
5	Build orientation	horizontal		vertical

Based on the five control factors a full factorial experimental plan of 32 parts was designed. Additionally 8 centre point parts were added to detect non-linearity and estimate error levels. All parts were produced using an SLM Solutions SLM280HL machine. Titanium alloy Ti6Al4V (grade 5) was selected as build material for its wide interest in aerospace, biomedical and industrial fields due to its fracture resistance, fatigue behaviour and corrosion resistance [18]. The build layer thickness was 50 µm. In Figure 1(a-b) the printed specimens are shown for the horizontally and vertically produced test sets, respectively.

a) 20 horizontal parts b) 20 vertical parts c) part geometry

Figure 1. SLM produced tensile test specimens.

After production, full annealing was performed at 735 °C for 2 h. Then, after fast cooling under a protective atmosphere, the parts were removed from the build plate. Thereafter the parts underwent a solution heat treatment (928 °C for 1 h) and aging heat treatment (538 °C for 3 h) followed by fast cooling under a protective atmosphere. Finally a post processing operation by machining was performed. All centre sections were Ø3 ±0.05 mm, the other geometries are specified in Figure 1(c).

4. Comparison of porosity testing methods

Tensile testing, Archimedes and microscopic analyses were conducted on all test parts. Six selected specimens were further analysed through gas pycnometry, CT, and additional sectioning and micrographing. Microscopic analyses were performed after tensile testing by cutting the much thicker section of the test part far away from the breakage point, thereby minimizing the influence of tensile testing. For CT, the relative porosity (complementary to relative density) was determined by the ratio of the total porosity volume to the total sample volume.

A new procedure aimed to compare microscopic analysis results with CT results was also developed. The specimen was CT scanned to identify the coordinates of a section of interest (e.g. a layer showing irregularities) before performing the cutting procedure. After the microscopic analysis of the obtained cross-section, a second CT scan was conducted on the cut part and a best fit alignment with the pre-cut scanned volume was addressed to identify the exact location of the cross-section in the pre-cut volume, where a 2D CT defect analysis was performed (same algorithm and thresholding parameters applied for the 3D defect analysis). Therefore, this paper distinguishes between CT results before and after the cutting and polishing operations; pre-cut and post-cut, respectively. Finally, specific pores lying on the cross-section of interest are measured using a high accuracy CMM equipped with image processing sensor (Werth Video-Check-IP 400; maximum permissible error equal to $(1.8+L/250)$ µm, with L in mm) to get reliable reference values for pore areas.

4.1. Relation between porosity and mechanical strength

First, the relation between part porosity and mechanical strength is determined. The tensile test results are compared to the porosity values of both the Archimedes method and the micrograph results. Figure 2 shows this comparison for the horizontally oriented parts. The two significant drops in both strength curves are detected by a porosity value larger than 1%. Hence, in this case both global and local testing methods are

predictive for static loading in-plane with the build layers. For loading perpendicular to the build layers (i.e. the vertically oriented parts) both methods are less predictive. This is likely due to the variation in tensile test results that are not as uniform as for the horizontally oriented parts. In both sets no. 17-20 are centre point parts and should therefore be similar. The standard deviations are 0.58 MPa (horizontal) and 17.7 MPa (vertical) showing 30x more deviation for vertical parts.

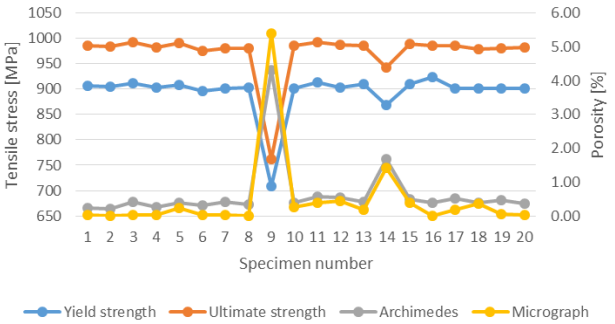

Figure 2. Tensile test results compared to Archimedes and micrograph porosity testing methods for the 20 horizontally oriented test specimens.

4.2. Volume-based testing methods comparison

Figure 3 shows the comparison between the Archimedes method and CT. The computed relative densities are reported on the left vertical axis. As visible, both methods are correlated; however, the Archimedes density is systematically lower than the density measured by CT. This is likely due to the inherent differences between the two testing methods. Archimedes can be considered accurate in absolute density measurements, but for deriving the relative density, as well as the porosity percentage, it is necessary to take the nominal density of Ti6Al4V (4.43 g/cm^3) as a reference. This reference, however, cannot be considered reliable for non-homogeneous parts. On the other hand, CT results are influenced by several image artefacts (e.g. due to X-ray beam hardening and scattering), by the achieved resolution (e.g. pores with sizes lower than the spatial resolution cannot be detected) and by the thresholding procedure. Further research work is needed to evaluate the measurement uncertainty of CT porosity analysis [19]. Finally, unmolten powder residue can be another source of diversity, as illustrated in Figure 4.

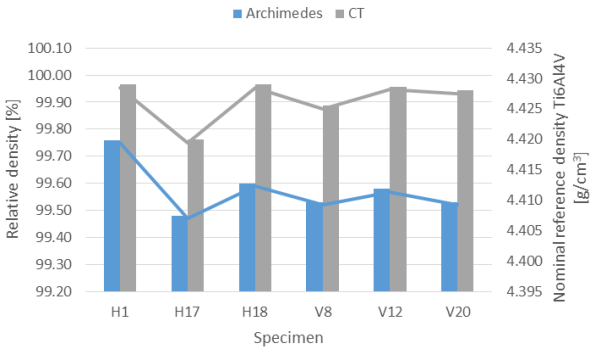

Figure 3. Comparison of Archimedes method and CT for density analysis.

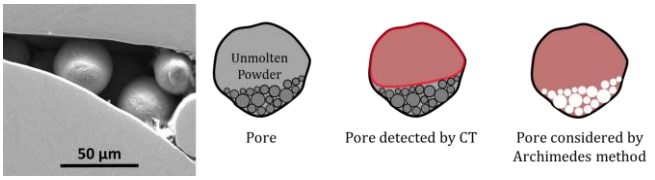

a) actual pore (part V20) b) detection differences

Figure 4. (a) SEM image of unmolten powder in a pore. (b) Illustration of the unmolten powder influence on pore detection for CT and Archimedes.

The pycnometer results are not reported in the comparison histogram. They are very scattered as the density measurements vary. This was confirmed in a second test at another laboratory. The disparity is likely due to insufficient accuracy for such small porosity percentages and due to the poor reliability of the nominal reference density for non-homogeneous parts.

The statistical analysis of the Archimedes method results showed that the control factors triggered significant effects, considering a significance level (p-value) of 5%. Also, the location of the test parts, determined by the *x* and *y* position on the build platform, showed not to be significant using the same p-value.

4.3. Area-based testing methods comparison

The comparison between CT and microscopic analysis results was conducted by following the aforementioned newly developed procedure. The diagram in Figure 5 shows the area measurements of 24 pores lying in one cross-section of Part H17, obtained by CT (pre-cut and post-cut), microscopic analysis and CMM equipped with a video sensor. Cross-sections on other specimens were analysed as well and confirmed these results.

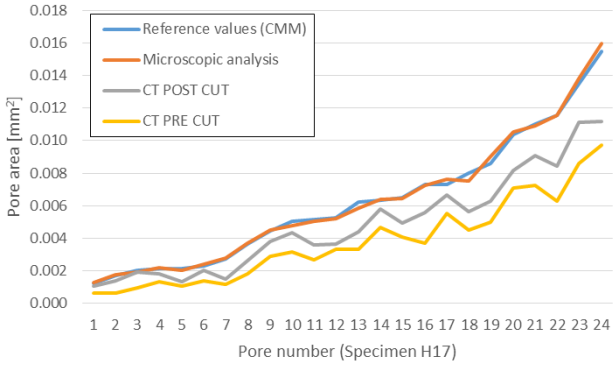

Figure 5. Pore size comparison for CMM, micrograph and pre/post-cut CT

The microscopic analysis results are close to the CMM results, while CT always measures smaller areas. This is visually confirmed by Figure 6, in which one micrograph is compared with the corresponding CT slice (pre-cut). Both optical techniques and CT are influenced by several factors which could partially explain the observed diversity. The CT main influences were already discussed in Section 4.2; while micrographs can be influenced by light and focus settings, stitching operations, thresholding and binarization. Other possible causes can be deformations due to cutting/polishing operations and the aforementioned presence of entrapped unmolten powder residue that may fall out during the cutting operation. These causes find an evidence in the difference between CT pre-cut and CT post-cut results. In particular, CT pre-cut area measurements are systematically lower compared to CT results obtained after cutting. A number of internal sections were compared as well to demonstrate that this difference regards only the cut sections.

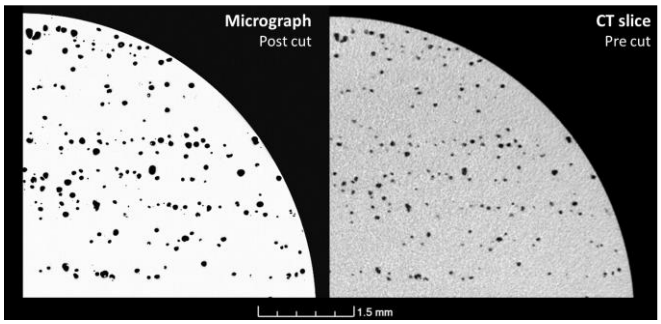

Figure 6. Comparison between post-cut micrograph and pre-cut CT.

5. Pore morphology and distribution analysis

Sphericity and elongation were introduced as indicators of the pore morphology. Considering two specimens as an example, Figure 7 shows Part H17 having much more pores with high sphericity than Part H18. This is visually confirmed by the cross-sections shown on the right of Figure 7. The average pore elongation per principle axis of these two specimens was also analysed. Part H17 has a smaller difference in average sizes between the three directions than Part H18, also confirming that pores in Part H17 are more spherical. For both parts the *x* and *y* sizes are larger than along the *z* axis, meaning pores tend to elongate in the *x-y* plane (i.e. the build platform plane). These differences, however, do not lead to a significant variation in tensile test results as was observed in Figure 2. The Archimedes results showed just a 0.1% higher relative porosity for Part H17.

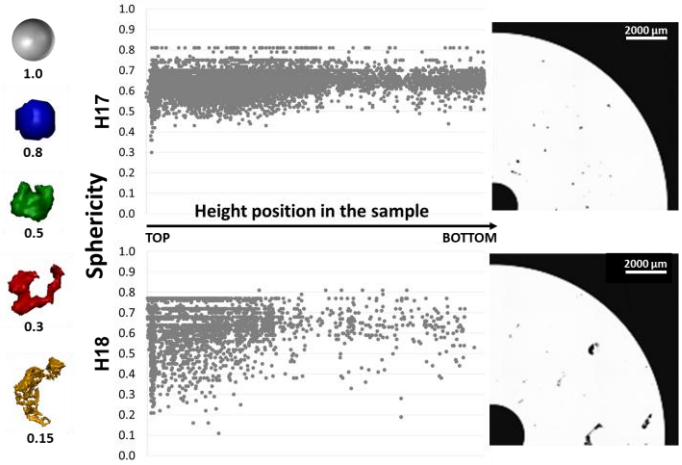

Figure 7. CT sphericity analysis showing the part's pore morphology.

Furthermore, with CT the pore distribution and location can be analysed and e.g. typical spiral staircase porosity distributions due to hatching errors in a continuously rotating laser scan projection can be detected. This can be easily observed in the CT reconstructed 3D volume of Part H17 (Figure 8).

Finally, CT gives the possibility of evaluating the volume of defects located on the external surface of a part as shown in Figure 9. To avoid nuclei for crack growth the surface finish should be smooth; however, this result shows that although post process machining is deployed, external defects are inevitable for SLM parts. Two centre point specimens (i.e. manufactured with the same process parameters) but with a different build orientation are compared: Part H17 and Part V20. The external porosity volume was found to be 6% and 12% with respect to the internal porosity volume, respectively. The higher percentage for the vertical specimen can also be traced back to the high variation in tensile test results, as discussed in Section 4.1.

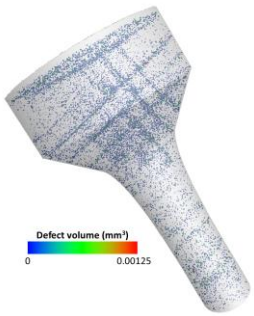

Figure 8. CT reconstructed 3D volume of Part H17 showing a staircase pore distribution.

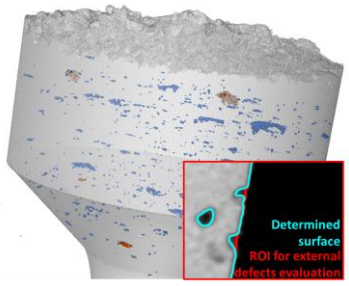

Figure 9. Detection of pores/defects on the external surface (in orange); internal pores are blue (Part V20).

6. Conclusions

Following an experimental plan, several destructive and non-destructive testing methods were compared. Density-based testing methods can be used for the evaluation of a global porosity percentage. Figures 2, 3 and 5 demonstrate that Archimedes, microscopic and CT methods show comparable trends for porosity prediction, although the predicted values may differ. Causes of differences were explained. Gas pycnometry proved not to be accurate enough for testing parts with porosity percentages lower than 0.5%, while the Archimedes method, being substantially less expensive, proved to be adequate to inspect parts in small series, identifying poor quality parts.

Furthermore, Archimedes results are comparable with CT results, although CT predicts systematically higher relative density values due to several causes, including the different measuring principle and the presence of unmolten powder residue. CT always measures pore areas smaller than microscopic methods. Among the several causes, the unmolten powder residue and the possible deformation due to cutting and polishing were confirmed by comparing CT results obtained before and after cutting: CT post-cut results are systematically higher than CT pre-cut results.

The added benefits of CT to investigate and quantify pore morphology, pore distribution and surface defects were shown in Chapter 5. Figures 7-9 show a non-uniform porosity distribution; however, this non-uniformity did not significantly influence the tensile testing results. The relation with other mechanical properties needs to be further investigated.

Acknowledgements

The authors kindly acknowledge the support of the Netherlands Aerospace Centre (NLR) for the SLM test part production and part of the experimental work. In particular, Marc de Smit and Lennart Terpstra are sincerely thanked.

References

[1] Levy, G.N., Schindel, R., Kruth, J.P., 2003, Rapid manufacturing and rapid tooling with layer manufacturing (LM) technologies, state of the art and future perspectives, CIRP Annals, 52/2: 589-609.
[2] Huis in 't Veld, B., et al., 2015, Micro additive manufacturing using ultra short laser pulses, CIRP Annals, 64/2: 701-724.
[3] Klocke, F., et al., 2014, Turbomachinery component manufacture by application of electrochemical, electrophysical and photonic processes, CIRP Annals 63:703-726.
[4] US NIST, 2013, Measurement science roadmap for metal-based AM.
[5] Frazier, W.E., 2014, Metal Additive Manufacturing: A Review, Journal of Materials Engineering and Performance, Vol. 23(6): 1917-1928.
[6] Yadroitsev, I., et al., 2010, Selective laser melting technology: from the single laser melted track stability to 3D parts of complex shape, Phys Procedia 5: 551–560.
[7] Wits W.W., et al., 2016, Single scan vector prediction in selective laser melting, Additive Manufacturing, Vol. 9: 1-6.
[8] Kempen, K., et al., 2011, Microstructure and mechanical properties of Selective Laser Melted 18Ni-300 steel, Physics Procedia, Vol. 12, Part A: 255-263.
[9] Vrancken B., et al., 2012, Heat treatment of Ti6Al4V produced by Selective Laser Melting: Microstructure and Mechanical properties, J Alloy Comp, 541(0): 177-185.
[10] Vilaro, T., et al., 2011, As-Fabricated and Heat-Treated Microstructures of the Ti-6Al-4V Alloy Processed by SLM, Metall Mater Trans A, 42: 3190–3199.
[11] Kruth, J.-P., et al., 2007, Consolidation phenomena in laserand powder-bed based layered manufacturing. CIRP Annals, 56/2: 730–759.
[12] Gong, H., et al., 2013, Defect Morphology in Ti-6Al-4V Parts Fabricated by SLM and EBM, 24rd Annual Int. Solid Freeform Fabrication: 440-453.
[13] Spierings, A.B., et al., 2011, Comparison of density measurement techniques for additive manufactured metallic parts, Rapid Prototyping Journal, 17(5): 380-386.
[14] Khademzadeh S., et al., 2016, Micro porosity analysis in additive manufactured NiTi parts using micro CT and electron microscopy. Materials & Design, 90: 745-752.
[15] Ontiveros S., et al., 2012, Dimensional measurement of micro-moulded parts by computed tomography. Measurement Science & Technology, 23: 125401.
[16] Yagüe-Fabra J.A., et al., 2013, A 3D edge detection technique for surface extraction in CT for dimensional metrology applications. CIRP Annals, 62/1:531-534.
[17] Carmignato S., 2012, Accuracy of industrial CT measurements: experimental results from an international comparison. CIRP Annals, 61/1: 491-494.
[18] Soboyejo, W.O., Srivatsan, T.S., 2006, Advanced Structural Materials: Properties, Design Optimization, and Applications, CRC Press: 359-400.
[19] Carmignato S., Savio E., 2011, Traceable volume measurements using coordinate measuring systems. CIRP Annals, 60/1: 519-522.